

Dissipative engineering a tripartite Greenberger-Horne-Zeilinger state for neutral atoms

D. X. Li,^{1,2} H. W. Xiao,^{1,2} C. Yang,^{1,2,*} and X. Q. Shao^{1,2,†}

¹Center for Quantum Sciences and School of Physics, Northeast Normal University, Changchun, 130024, China

²Center for Advanced Optoelectronic Functional Materials Research,
and Key Laboratory for UV Light-Emitting Materials and Technology of Ministry of Education,
Northeast Normal University, Changchun 130024, China

(Dated: April 27, 2020)

The multipartite Greenberger-Horne-Zeilinger (GHZ) states are indispensable elements for various quantum information processing tasks. Here we put forward two deterministic proposals to dissipatively prepare tripartite GHZ states in a neutral atom system. The first scheme can be considered as an extension of a recent work [T. M. Wintermantel, Y. Wang, G. Lochead, *et al.*, *Phys. Rev. Lett.* **124**, 070503 (2020)]. By virtue of the polychromatic driving fields and the engineered spontaneous emission, a multipartite GHZ state with odd numbers of atoms are generated with a high efficiency. This scheme effectively overcomes the problem of dependence on the initial state but sensitive to the decay of Rydberg state. In the second scenario, we exploit the spontaneous emission of the Rydberg states as a resource, thence a steady tripartite GHZ state with fidelity around 98% can be obtained by simultaneously integrating the switching driving of unconventional Rydberg pumping and the Rydberg antiblockade effect.

I. INTRODUCTION

Neutral atoms excited to Rydberg states own strong, controllable Rydberg-mediated interactions that make Rydberg-atom systems become one of the most promising and versatile platforms in the fields of quantum information processing [1], quantum optics [2, 3], quantum many-body physics [4–6], and quantum metrology [7–10]. This exotic feature has been intensively explored and several milestones have been put forward. A prominent example is the Rydberg blockade. Benefitting from the significant suppression of the simultaneous excitation for Rydberg atoms, it serves as the backbone not only for a two qubit controlled phase gate [1, 11, 12], but also for entanglement generation [13–16], quantum algorithms [17], quantum simulators [4], and quantum repeaters [18]. On the other hands, an opposite effect, the Rydberg antiblockade [19, 20], also sheds new light on fundamental questions about quantum logic gate [21, 22], preparations of quantum entanglement [23–26], and directional quantum state transfer [27]. It is induced by combining Rydberg interactions with the two-photon detuning to realize the simultaneous excitation of two Rydberg atoms. With the rapid development of quantum information, entanglement in bipartite systems has been well understood and quantified [28]. More and more researchers begin to focus on unleashing the potential of multipartite entanglement in the context of measurement-based quantum computation [29–31], quantum error correction [32, 33], quantum networks [34–36], and condensed matter physics [37, 38]. Compared with bipartite entanglement, multipartite entanglement is more powerful to manifest the nonlocality of quantum physics [28, 39].

As a representative genuine multipartite entanglement, GHZ states [40] enable a new understanding to research the local and realistic worldview further with more refined

demonstrations of quantum nonlocality. Besides, they supply efficient manners for large-scale cluster state generation of measurement-based quantum computing [41, 42], quantum metrology [43–45], and high-precision spectroscopy [46, 47]. Therefore, the preparation and measurement of GHZ states via diverse systems have been sought for a long time and remains an attractive field of research. Nowadays, a myriad of theoretical and experimental literatures to generate GHZ states have been proposed [48–51]. Particularly in Ref. [49], the authors presented a dissipative scheme to prepare a GHZ state of three Rydberg atoms in a cavity. Although they united quantum Zeno dynamics with Rydberg antiblockade effect to depress the harmful effect from the cavity, guaranteeing the high quality of a cavity is still a challenge in experiments, and the Rydberg atoms trapped into a cavity pronouncedly increase the experimental difficulties.

Quite recently, integrating the Rydberg interactions and dichromatic driving fields, our group [52] discovered another fantastic effect, unconventional Rydberg pumping (URP), which is ground-state-dependent and differs from the general Rydberg blockade or antiblockade. It will freeze the system consisting of two atoms at the same ground state and excite the system with two atoms at different ground states. The remarkable effect has exhibited the spectacular potential for various quantum information processing tasks, such as the achievement of quantum logic gate and the generation of entangled states. Furthermore, it is a meritorious pillar-stone to perform the autonomous quantum error correction for avoiding the bit-flip error of GHZ states in quantum metrology. Additionally, analogous to the dichromatic driving fields of URP, Wintermantel *et al.* [53] recently introduced programmable multifrequency couplings in arrays of Rydberg atoms to generalize the Rydberg blockade effect and nonunitarily prepare GHZ states. However, the corresponding system has to be comprised of even numbers of atoms, and the optimal parameters cannot guarantee a unique steady-state solution of system. For instance, the target GHZ state $(|0\rangle^{\otimes 4} + |1\rangle^{\otimes 4})/\sqrt{2}$ or $(|0\rangle^{\otimes 6} - |1\rangle^{\otimes 6})/\sqrt{2}$ cannot be implemented from the initial states in the basis of $\{|1100\rangle, |0110\rangle, |0011\rangle\}$ or $\{$

* yangc812@nenu.edu.cn

† shaoxq644@nenu.edu.cn

$|110000\rangle, |110100\rangle, |110110\rangle, |111100\rangle\}$.

Since the tripartite GHZ state is the simplest GHZ state manipulated in an experiment, and the disturbances of next-nearest neighbor Rydberg atoms can be circumvented excellently in a three-particle system, we propose two reliable schemes to dissipatively achieve the tripartite GHZ state in this paper. Our first proposal unites the polychromatic driving fields and engineered spontaneous emissions of a short-lived level to realize the dissipative preparation of a tripartite GHZ state, which can significantly compensate for the problem of dependence on the initial state. Nevertheless, once the spontaneous emission of the Rydberg state is accessed, the population of the tripartite GHZ state will steeply descend. Thus, we design the second dissipative scheme that turns the Rydberg state decay into an important resource. The decay cooperating with the switching driving of URP and the Rydberg antiblockade successfully generates the tripartite GHZ state with a high fidelity around 98%. As the target state is the unique steady state of the whole system, this scheme is also independent of the certain transport time and the tailored initial state, which is the feature of dissipative entangled-state preparations. In what follows, we will interpret in detail the principle of the above operations.

II. SCHEME BASED ON POLYCHROMATIC DRIVING FIELDS

A. Physical mechanism and effective dynamics

The setup and the corresponding atomic energy levels of the scheme based on the polychromatic driving fields and the engineered spontaneous emission are illustrated in Fig. 1. We assume three identical Rydberg atoms, all consisting of a ground state $|g\rangle$, a Rydberg state $|r\rangle$, and a temporary (short-lived) level $|e\rangle$, interact with the polychromatic driving fields $\Omega_{1,2,3}$ and a classical laser Ω_0 . While the polychromatic driving fields $\Omega_{1,2,3}$ respectively drive the transitions $|g\rangle \leftrightarrow |r\rangle$ with detunings $-\Delta_{1,2,3}$, the classical laser Ω_0 resonantly couples the short-lived state $|e\rangle$ with the Rydberg state $|r\rangle$.

Supposing the three atoms decay from the short-lived state $|e\rangle$ to the ground state $|g\rangle$ with the same spontaneous emission rate Γ , the full master equation in the interaction picture can be written as

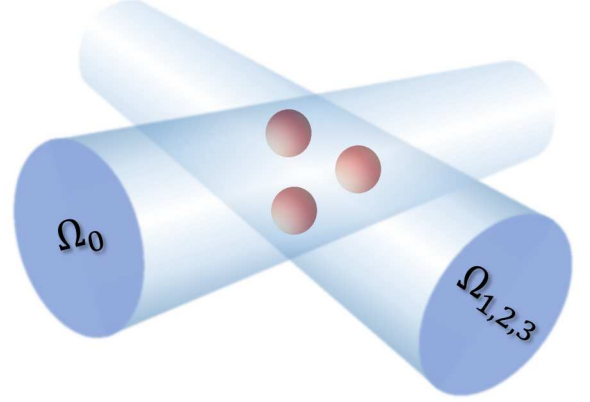
$$\dot{\rho} = -i[H, \rho] + \sum_{j=1}^3 L_j \rho L_j^\dagger - \frac{1}{2}(L_j^\dagger L_j \rho + \rho L_j^\dagger L_j), \quad (1)$$

where

$$H = \sum_{j,\alpha} \Omega_\alpha \sigma_j^{r\alpha} e^{-i\Delta_\alpha t} + \Omega_0 \sigma_j^{re} + \text{H.c.} + \sum_{k>j} U_{jk} \sigma_j^{rr} \sigma_k^{rr},$$

and $L_j = \sqrt{\Gamma} \sigma_j^{ge}$. Here $|x\rangle_j \langle y|$ is parametrized as σ_j^{xy} . And U_{jk} bridges the Rydberg interaction, caused by the dipole-dipole potential or the long-range van der Waals interaction, between the j - and k -th Rydberg atoms, which can obey the relation $U_{12} = U_{23} = U_{13} = U$ through the appropriate

Setup



Atomic levels

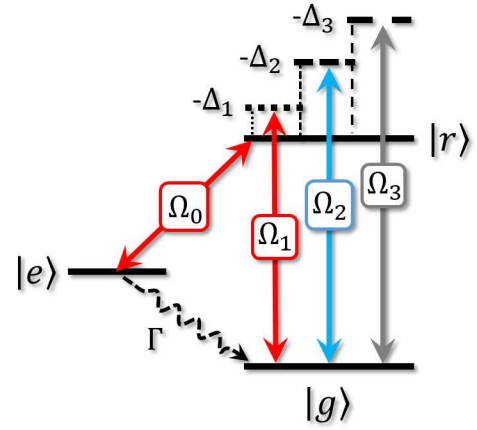


FIG. 1. The setup for the scheme based on the polychromatic driving fields and the engineered spontaneous emission, and the diagram of corresponding atomic energy levels. Three Rydberg atoms interact with the polychromatic driving fields $\Omega_{1,2,3}$ and a classical laser Ω_0 .

adjustments of the interatomic distance and the atomic principal quantum numbers [54, 55]. Since the lifetime of the temporary state $|e\rangle$ is short, we consider the decay rate Γ is much greater than the coupling strength Ω_0 , *i.e.*, $\Gamma \gg \Omega_0$. And in the limiting condition of $U \gg \Omega_{0,1,2,3}$, we can reformulate the Hamiltonian in a rotating frame with respect to $U_0 = \exp\{-it \sum_{k>j} U_{jk} \sigma_j^{rr} \sigma_k^{rr}\}$,

$$H_I = H_r + H_e, \quad (2)$$

with

$$H_r = \sum_{j,m,n} 2^{|m-n|} \Omega_{m+n+1} P_{j-1}^{m} \sigma_j^{rg} P_{j+1}^n e^{i(m+n-1)\Delta_1 t} + \text{H.c.},$$

$$H_e = \sum_j \Omega_0 P_{j-1}^0 \sigma_j^{er} P_{j+1}^0 + \text{H.c.},$$

where $m, n = 0, 1$, $P_j^0 = |g\rangle_j \langle g|$, $P_j^1 = |r\rangle_j \langle r|$, periodic boundary conditions of j is considered, and we have set $U =$

$\Delta_2 = (\Delta_3 + \Delta_1)/2$ and $\Delta_1 = 2\Omega_2$ to achieve the Rydberg antiblockade effect. As for the other terms, we have neglected them as the large detuning conditions and the short lifetime of state $|e\rangle$.

The corresponding operators of atomic spontaneous emission can be simplified as $L^{(j)} = \sqrt{\Gamma}P_{j-1}^0\sigma_j^{ge}P_{j+1}^0$. Then we can adiabatically eliminate the state $|e\rangle$ to obtain an engineered spontaneous emission. For the sake of a clear show about the mechanism, we discard the effective Hamiltonian H_r , and take the Hamiltonian $\Omega_0\sigma_1^{er}P_2^0P_3^0 + \text{H.c.}$ of H_e and the effective Lindblad operator $L^{(1)}$ as an example. A reduced master equation reads

$$\begin{aligned} \dot{\rho}_e = & -i[\Omega_0\sigma_1^{er}P_2^0P_3^0 + \text{H.c.}, \rho_e] \\ & + L^{(1)}\rho_e L^{(1)\dagger} - \frac{1}{2}(L^{(1)\dagger}L^{(1)}\rho_e + \rho_e L^{(1)\dagger}L^{(1)}). \end{aligned} \quad (3)$$

The density operator can be written in the basis of $\{|ggg\rangle, |egg\rangle, |rgr\rangle\}$ as

$$\rho_e = \begin{pmatrix} \rho_{gg} & \rho_{ge} & \rho_{gr} \\ \rho_{eg} & \rho_{ee} & \rho_{er} \\ \rho_{rg} & \rho_{re} & \rho_{rr} \end{pmatrix}. \quad (4)$$

Substituting it into the Eq. (3), we can obtain a set of coupled equations for the matrix elements

$$\dot{\rho}_{gg} = \Gamma\rho_{ee}, \quad (5)$$

$$\dot{\rho}_{ge} = i\Omega_0\rho_{gr} - \frac{\Gamma}{2}\rho_{ge}, \quad (6)$$

$$\dot{\rho}_{gr} = i\Omega_0\rho_{ge}, \quad (7)$$

$$\dot{\rho}_{ee} = i\Omega_0(\rho_{er} - \rho_{re}) - \Gamma\rho_{ee}, \quad (8)$$

$$\dot{\rho}_{er} = i\Omega_0(\rho_{ee} - \rho_{rr}) - \frac{\Gamma}{2}\rho_{er}, \quad (9)$$

$$\dot{\rho}_{rr} = i\Omega_0(\rho_{re} - \rho_{er}). \quad (10)$$

In the limit of $\Gamma \gg \Omega_0$, it is reasonable to presume $\dot{\rho}_{ge} = \dot{\rho}_{ee} = \dot{\rho}_{er} = 0$. We can solve that $\rho_{ge} = 2i\Omega_0\rho_{gr}/\Gamma$, $\rho_{er} = -2i\Omega_0\rho_{rr}/(\Gamma^2 + 4\Omega_0^2)$, and $\rho_{ee} = 4\Omega_0^2\rho_{rr}/(\Gamma^2 + 4\Omega_0^2)$. Then the coupled equations of the matrix elements can be rewritten as

$$\dot{\rho}_{gg} = -\dot{\rho}_{gg} = \Gamma_{\text{eff}}\rho_{rr}, \quad \rho_{gr} = -\frac{\Gamma_{\text{eff}}}{2}\rho_{gr}, \quad \Gamma_{\text{eff}} = \frac{4\Omega_0^2}{\Gamma}.$$

Then Eq. (3) can be derived as

$$\dot{\rho}_e = L_{\text{eff}}^1\rho_e L_{\text{eff}}^{1\dagger} - \frac{1}{2}(L_{\text{eff}}^{1\dagger}L_{\text{eff}}^1\rho_e + \rho_e L_{\text{eff}}^{1\dagger}L_{\text{eff}}^1), \quad (11)$$

where $L_{\text{eff}}^1 = \sqrt{\Gamma_{\text{eff}}}\sigma_1^{gr}P_2^0P_3^0$. The other terms of H_e and the Lindblad operators $L^{(2,3)}$ can be simplified via the similar method. Thus, the total system can be equivalent to

$$\dot{\rho} = -i[H_r, \rho] + \sum_j L_{\text{eff}}^j\rho L_{\text{eff}}^{j\dagger} - \frac{1}{2}(L_{\text{eff}}^{j\dagger}L_{\text{eff}}^j\rho + \rho L_{\text{eff}}^{j\dagger}L_{\text{eff}}^j),$$

where $L_{\text{eff}}^j = \sqrt{\Gamma_{\text{eff}}}\sigma_{j-1}^0\sigma_j^{gr}P_{j+1}^0$ is the engineered spontaneous emission.

To further describe the principle of this scheme, we can diagonalize the resonant terms of H_r and get that

$$\begin{aligned} H_r = & \sqrt{3}\Omega(|\text{GHZ}_+\rangle\langle E_{1+}| + |\text{GHZ}_-\rangle\langle E_{1-}|)e^{i\Delta_1 t} + \text{H.c.} \\ & + \Omega_2(2|E_{1+}\rangle\langle E_{1+}| - 2|E_{1-}\rangle\langle E_{1-}| + |E_{2+}\rangle\langle E_{2+}| \\ & - |E_{2-}\rangle\langle E_{2-}| + |E_{3+}\rangle\langle E_{3+}| - |E_{3-}\rangle\langle E_{3-}|), \end{aligned} \quad (12)$$

where we set $\Omega_1 = \Omega_3 = \Omega$ for simplicity and have abbreviated $|\text{GHZ}_{\pm}\rangle = (|ggg\rangle \pm |rrr\rangle)/\sqrt{2}$, $|E_{1\pm}\rangle = (|grr\rangle + |rgr\rangle + |rrg\rangle \pm |ggr\rangle \pm |grg\rangle \pm |rgg\rangle)/\sqrt{6}$, $|E_{2\pm}\rangle = (|rrg\rangle - |grr\rangle \pm |rgr\rangle \mp |ggr\rangle)/2$, and $|E_{3\pm}\rangle = (2|rgr\rangle - |grr\rangle - |rrg\rangle \mp 2|grg\rangle \pm |ggr\rangle \pm |rgg\rangle)/2\sqrt{3}$. We can find that the Hamiltonian of Eq. (12) reveals the dispersive transitions of $|\text{GHZ}_{\pm}\rangle \leftrightarrow |E_{1\pm}\rangle$ with detuning $\Delta_1 \mp 2\Omega_2$. (Note that for the system consists of even numbers of atoms [53], there is a resonant transition between $|\text{GHZ}_+\rangle$ or $|\text{GHZ}_-\rangle$ and a certain dark state in the presence of $\Delta_1 = 0$.) Once we assume $\Delta_1 = 2\Omega_2$, $\Omega_2 \gg \Omega$ and rotate the above Hamiltonian with $\exp\{-2i\Omega_2 t(|E_{1+}\rangle\langle E_{1+}| - |E_{1-}\rangle\langle E_{1-}|)\}$, the effective Hamiltonian based on the polychromatic driving fields can amount to

$$\begin{aligned} H_{\text{eff}} = & \sqrt{3}\Omega|\text{GHZ}_+\rangle\langle E_{1+}| + \text{H.c.} + \Omega_2(|E_{2+}\rangle\langle E_{2+}| \\ & - |E_{2-}\rangle\langle E_{2-}| + |E_{3+}\rangle\langle E_{3+}| - |E_{3-}\rangle\langle E_{3-}|) \end{aligned} \quad (13)$$

where the term of $|\text{GHZ}_-\rangle\langle E_{1-}| + \text{H.c.}$ have been omitted as the corresponding large detuning is $4\Omega_2$ and only the resonant transition of $|\text{GHZ}_+\rangle \leftrightarrow |E_{1+}\rangle$ remains. Then the effective master equation of the whole system reads

$$\dot{\rho} = -i[H_{\text{eff}}, \rho] + \sum_j L_{\text{eff}}^j\rho L_{\text{eff}}^{j\dagger} - \frac{1}{2}(L_{\text{eff}}^{j\dagger}L_{\text{eff}}^j\rho + \rho L_{\text{eff}}^{j\dagger}L_{\text{eff}}^j), \quad (14)$$

According to the Eq. (14), the target state $|\text{GHZ}_-\rangle$ is the unique steady-state solution of this model, *i.e.*, $H_{\text{eff}}|\text{GHZ}_-\rangle = L_{\text{eff}}^j|\text{GHZ}_-\rangle = 0$. Therefore, initialized at an arbitrary state, the system can be stabilized at $|\text{GHZ}_-\rangle$.

B. Numerical results

In Fig. 2, we plot the dynamical evolution for the populations of the target state $|\text{GHZ}_-\rangle$ governed by the full master equation Eq. (1) (solid line) and the effective master equation Eq. (14) (empty circles), respectively. The brilliant agreement of the two curves adequately proves the validity of the reduced system. It is significant to forecast and interpret the behaviors of the original system. Furthermore, the populations of $|\text{GHZ}_+\rangle$ (dashed line) and $|\text{GHZ}_-\rangle$ are respectively stable at 0.30% and 99.54% with the time just at $200/\Omega_2$, which reflects the feasibility and the high efficiency of the first dissipative scheme. The initial state is chosen as a mixed state $\rho_0 = \sum_{l,m,n} P_1^l P_2^m P_3^n / 8$ ($l, m, n = 0, 1$). It means the target state is the unique steady state of the whole system, and this is also one of the remarkable features of dissipative entangled-state preparations. Additionally, stimulated by this principle, the present scheme can be generalized to prepare an arbitrary

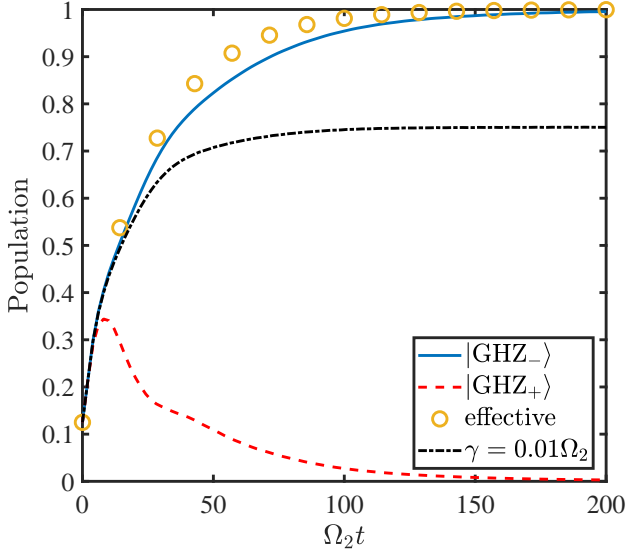


FIG. 2. The population of different states as functions of $\Omega_2 t$. The definition of the population for the state $|i\rangle$ is $P_i = \langle i|\rho(t)|i\rangle$. The initial states are all chosen as a mixed state $\rho_0 = \sum_{l,m,n} P_1^l P_2^m P_3^n / 8$ ($l, m, n = 0, 1$). The other parameters are $\Omega_0 = 0.77\Omega_2$, $\Omega_1 = \Omega_3 = 0.05\Omega_2$, $\Gamma = 6\Omega_2$, and $U = 300\Omega_2$.

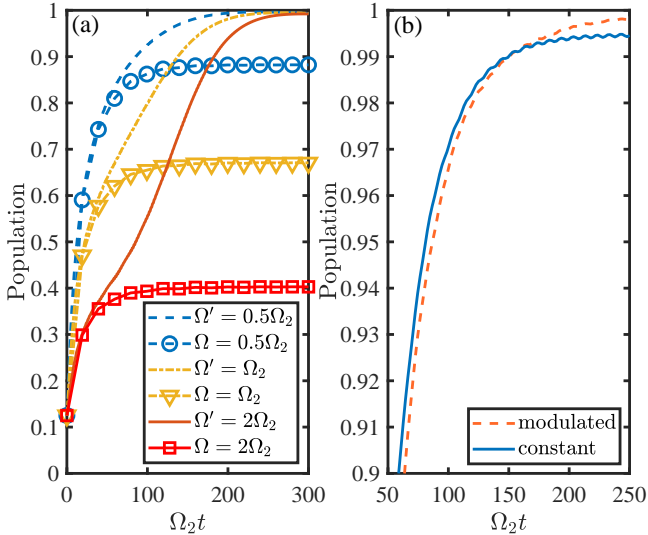


FIG. 3. The dynamical evolution for the population of $|GHZ_-\rangle$ with different modulated and constant coupling strengths. The initial states and the other parameters are all the same as those of Fig. 2 except for (a) $\sigma = 90/\Omega_2$, $\mu = 0$ and (b) $\Omega = \Omega' = 0.1\Omega_2$, $\sigma = 90/\Omega_2$, $\mu = 110/\Omega_2$.

multipartite GHZ state with odd numbers of atoms (see the Sec. IV for detail).

In order to release the restrictive condition $\Omega_2 \gg \Omega_{1,3}$, we also introduce the Gaussian pulse to improve this scheme. The key ingredient is a modulation for $\Omega_{1,3}$. In other words, the constant coupling strength $\Omega_{1,3} = \Omega$ need to be replaced into

$\Omega_{1,3}(t) = \Omega' \exp[-(t - \mu)^2 / (2\sigma^2)]$. Then the limiting condition of $\Omega_2 \gg \Omega_{1,3}$ is no longer necessary so long as we select suitable values of Ω' , σ , and μ . In Fig. 3(a), we depict the populations of $|GHZ_-\rangle$ with the polychromatic driving fields respectively applying the different modulated couplings and the corresponding constant couplings ($\Omega = \Omega'$). Owing to the Gaussian pulse, when the limiting condition $\Omega_2 \gg \Omega_{1,3}$ is violated, the populations of $|GHZ_-\rangle$ with the former still reach 99.27% (dashed line), 99.35% (dash-dotted line), and 99.21% at $\Omega_2 t = 300$. By contrast, those with the latter markedly decrease to 88.23% (empty circles), 67.07% (empty triangles), and 40.29% (empty squares). On the other hand, in Fig. 3(b), when we choose $\Omega' = 0.1\Omega_2$, $\sigma = 90/\Omega_2$, and $\mu = 110/\Omega_2$, the population of $|GHZ_-\rangle$ can be raised from 99.46% (solid line) to 99.81% (dashed line) at $\Omega_2 t = 250$. This performance manifests that the Gaussian pulse can promote the quality of the target state even though the limiting condition is not violated.

Although the efficiency is excellent, the present scheme is sensitive to the atomic spontaneous emission of the Rydberg state $|r\rangle$, which can be described by the Lindblad operators $L_j^r = \sqrt{\gamma}\sigma_j^{gr}$ (γ stands for the decay rate). Once we add L_j^r with γ just identical to $0.01\Omega_2$ into the Eq. (1), the population of the target state will steeply descend from 99.54% to 75.79% at $\Omega_2 t = 200$, which has been represented by the dash-dotted line in Fig. 2. And this disadvantage is not solved in the Ref. [53], either. Consequently, we devise the second scheme based on the switching driving of URP and the Rydberg antiblockade to change the role of the Rydberg state decay into a useful resource.

III. SCHEME BASED ON SWITCHING DRIVING FIELDS

Switching driving field is a good candidate to perfectly realize an ideal quantum process that cannot be performed by the natural evolution of systems. This technology has been used to advantage in an enormous amount of ingenious efforts, such as the implementation of quantum logic gates [56–58], the derivation and applications of the Trotter product formula $\exp\{\mathcal{L}t\} = \lim_{N \rightarrow \infty} (\exp\{\mathcal{L}_a t/N\} \exp\{(\mathcal{L} - \mathcal{L}_a)t/N\})^N$ [59–61], the preparation of entanglement with trapped ions [62, 63], and so on [64–66]. In this section, we will explicate the second scheme based on the switching driving of URP in detail.

A. Physical mechanism and effective dynamics

For this scheme, the system is constituted by three four-level Rydberg atoms that all encompass two ground states $|0\rangle$, $|1\rangle$ (encoded quantum bits), and two Rydberg states $|r\rangle$, $|p\rangle$. The corresponding flow chart has been elaborated in Fig. 4. It can be separated into two simultaneous processes to nonunitarily generate tripartite GHZ state $|GHZ_-\rangle = (|000\rangle - |111\rangle)/\sqrt{2}$ with an arbitrary initial state. One of the processes uses the switching driving of URP to transform the states with one or two atoms in state $|0\rangle$ into the subspace

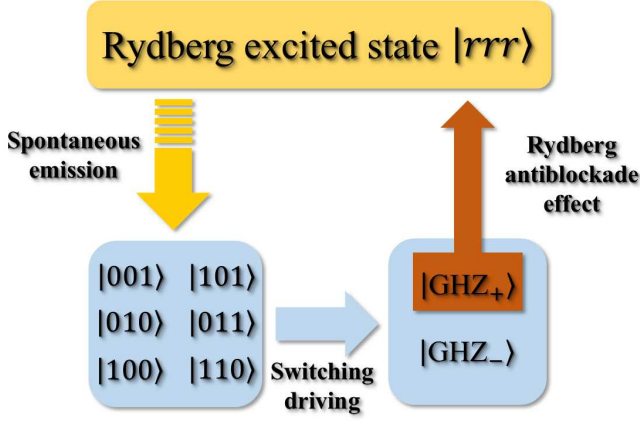


FIG. 4. Flow chart of the scheme based on the switching driving of URP and the Rydberg antiblockade.

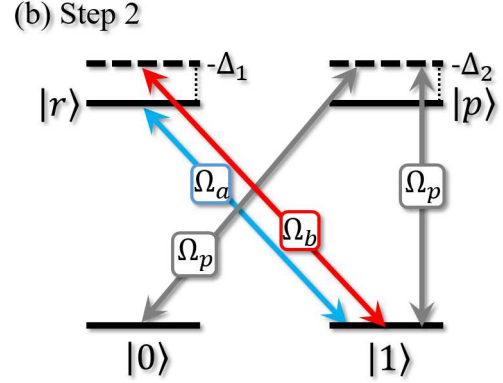
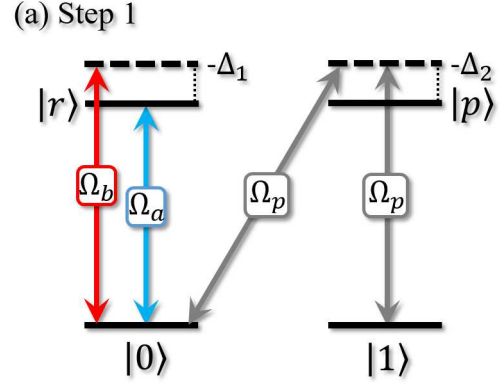
spanned by $|000\rangle$ and $|111\rangle$, which can be also expanded via $\{|GHZ_+\rangle, |GHZ_-\rangle\}$ as $|000\rangle = (|GHZ_+\rangle + |GHZ_-\rangle)/\sqrt{2}$ and $|111\rangle = (|GHZ_+\rangle - |GHZ_-\rangle)/\sqrt{2}$. In order to stabilize the system at the target state $|GHZ_-\rangle$, the other process capitalizes on the Rydberg antiblockade effect exciting the state $|+++ \rangle$ to the Rydberg excited state $|rrr\rangle$, and the stabilization of $|GHZ_+\rangle = (|+++ \rangle + |+- - \rangle + |-+- \rangle + |--+ \rangle)/2$ ($|\pm\rangle = (|0\rangle \pm |1\rangle)/\sqrt{2}$) can be destroyed. Subsequently, the state $|rrr\rangle$ will further decay to the ground states by the Rydberg state decay. The two simultaneous processes create a cycle among all states except $|GHZ_-\rangle$ and lead to the system steady at $|GHZ_-\rangle$ finally.

In Fig. 5(a) and 5(b), we flesh out the atomic levels in more detail. The process based on the switching driving of URP composes of the Step 1 and the Step 2 carried out alternately. For the Step 1, there are dichromatic driving fields with Rabi frequency Ω_a and Ω_b resonantly and dispersively (detuning $-\Delta_1$) driving the transitions $|r\rangle \leftrightarrow |0\rangle$. For the Step 2, the two lasers are switched to coupling the transitions $|r\rangle \leftrightarrow |1\rangle$ resonantly and dispersively. In the meantime, the process based on the Rydberg antiblockade effect will continuously accomplish the transitions $|p\rangle \leftrightarrow |0\rangle$ and $|p\rangle \leftrightarrow |1\rangle$ with two lasers (Rabi frequencies Ω_p , detunings $-\Delta_2$) regardless of which Step is in action. Moreover, we consider the Rydberg state $|r(p)\rangle$ decays to the ground states with the same rate $\gamma_{r(p)}/2$, and in what follows we set $\gamma_r = \gamma_p = \gamma$. In Fig. 5(c), we also depict the temporal schematic of the alternate operations to further clarify the scheme. In the interaction picture, the full master equation for the two steps can be written as

$$\dot{\rho} = -i[H_{S1} + H_p, \rho] + \mathcal{L}\rho, \quad (15)$$

and

$$\dot{\rho} = -i[H_{S2} + H_p, \rho] + \mathcal{L}\rho, \quad (16)$$



(c) Temporal schematic

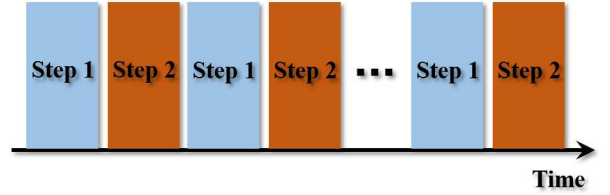


FIG. 5. (a) and (b) Atomic level configuration of the scheme based on the switching driving of URP and the Rydberg antiblockade, where the Step 1 and Step 2 will be carried out alternately during the whole process. The Rydberg state decays from $|r(p)\rangle$ to the ground states $|0\rangle$ and $|1\rangle$ with the same rate $\gamma_{r(p)}/2$ are not shown in the figures. (c) Temporal schematic for the alternate operations. The URP is switched frequently between the two steps, while the Rydberg antiblockade is in action all the time.

with

$$H_{S1(2)} = \sum_{j=1}^3 (\Omega_a + \Omega_b e^{-i\Delta t}) \sigma_j^{r0(1)} + \text{H.c.} + \sum_{j<k} U_{rr} \sigma_j^{rr} \sigma_k^{rr},$$

$$H_p = \sum_{j=1}^3 \sqrt{2} \Omega_p \sigma_j^{p+} e^{-i\Delta t} + \text{H.c.} + \sum_{j<k} U_{pp} \sigma_j^{pp} \sigma_k^{pp},$$

$$\mathcal{L}\rho = \sum_{\alpha=1}^4 \sum_{j=1}^3 L_j^\alpha \rho L_j^{\alpha\dagger} - \frac{1}{2} (L_j^{\alpha\dagger} L_j^\alpha \rho + \rho L_j^{\alpha\dagger} L_j^\alpha),$$

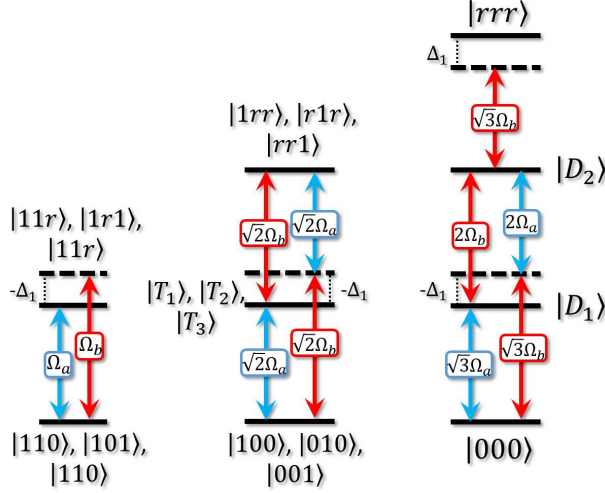


FIG. 6. The corresponding collective three-atom energy levels and transitions of Eq. (17).

where the Rydberg interaction of both atoms at $|r(p)\rangle$ is described by $U_{rr(pp)}$, the Rydberg interactions of two atoms occupying different Rydberg states can be ignored by means of regulating the interatomic distance and the atomic principal quantum numbers [54, 55], and the Lindblad operators are $L_j^{1(2)} = \sqrt{\gamma/2}\sigma_j^{0(1)r}$ and $L_j^{3(4)} = \sqrt{\gamma/2}\sigma_j^{0(1)p}$.

For completeness, here we briefly reproduce some results on the URP of Ref. [52] that are essential to understand our computational scheme. Referring to the conditions of the URP, we can take into account the $U_{rr} = \Delta_1$ and rotate the H_{S1} with $\exp\{-it \sum_{j < k} U_{rr} \sigma_j^{rr} \sigma_k^{rr}\}$. In the large-detuning regime, the H_{S1} can be divided into

$$H_{S1} = H_{S1}^1 + H_{S1}^2 + H_{S1}^3, \quad (17)$$

with

$$\begin{aligned} H_{S1}^1 &= \Omega_a(|110\rangle\langle 11r| + |101\rangle\langle 1r1| + |011\rangle\langle r11| + \text{H.c.}), \\ H_{S1}^2 &= \sqrt{3}\Omega_a|000\rangle\langle D_1| + 2\Omega_b|D_1\rangle\langle D_2| + \sqrt{2}\Omega_a(|100\rangle\langle T_1| \\ &\quad + |010\rangle\langle T_2| + |001\rangle\langle T_3|) + \sqrt{2}\Omega_b(|1rr\rangle\langle T_1| + |r1r\rangle \\ &\quad \otimes \langle T_2| + |rr1\rangle\langle T_3|) + \text{H.c.}, \\ H_{S1}^3 &= \left[\Omega_b(|110\rangle\langle 11r| + |101\rangle\langle 1r1| + |011\rangle\langle r11|) + \sqrt{2}\Omega_b \right. \\ &\quad (|100\rangle\langle T_1| + |010\rangle\langle T_2| + |001\rangle\langle T_3|) + \sqrt{2}\Omega_a(|1rr\rangle \\ &\quad \otimes \langle T_1| + |r1r\rangle\langle T_2| + |rr1\rangle\langle T_3|) + \sqrt{3}\Omega_b(|000\rangle\langle D_1| \\ &\quad \left. + |rrr\rangle\langle D_2|) + 2\Omega_a|D_2\rangle\langle D_1| \right] e^{i\Delta_1 t} + \text{H.c.}, \end{aligned}$$

where $|D_1\rangle = (|00r\rangle + |0r0\rangle + |r00\rangle)/\sqrt{3}$, $|D_2\rangle = (|0rr\rangle + |r0r\rangle + |rr0\rangle)/\sqrt{3}$, $|T_1\rangle = (|10r\rangle + |1r0\rangle)/\sqrt{2}$, $|T_2\rangle = (|01r\rangle + |r10\rangle)/\sqrt{2}$, and $|T_3\rangle = (|0r1\rangle + |r01\rangle)/\sqrt{2}$. To express these interactions visually, we exhibit the corresponding collective three-atom energy levels and transitions of Eq. (17)

in Fig. 6. The ground states will be resonantly and dispersively excited to the single excited states except for the ground state $|111\rangle$ which is not evolved via H_{S1} . The single excited states $|T_1\rangle$, $|T_2\rangle$, $|T_3\rangle$, and $|D_1\rangle$ can be resonantly and dispersively pumped to the corresponding double excited states $|11r\rangle$, $|r1r\rangle$, $|rr1\rangle$, and $|D_2\rangle$, where the double excited state $|D_2\rangle$ will be further transferred to $|rrr\rangle$ dispersively.

In the limit of $\Delta_1 \gg \Omega_b \gg \Omega_a$, H_{S1}^3 can approximate to the combination between the Stark-shift terms and the equivalent direct transitions from the ground states with three or two atoms at $|0\rangle$ to the corresponding double excited states. Moreover, the Stark-shift terms with the order of Ω_b^2/Δ_1 can be canceled out utilizing the other ancillary levels, while the other terms with the orders of Ω_a^2/Δ_1 and $\Omega_a\Omega_b/\Delta_1$ can be ignored as $\Omega_b \gg \Omega_a$. Consequently, H_{S1}^3 is useless for the scheme.

Then we can rewrite the H_{S1}^2 by diagonalizing the terms of Ω_b , and

$$\begin{aligned} H_{S1}^2 &= \sqrt{\frac{3}{2}}\Omega_a|000\rangle(\langle D_+| + \langle D_-|) + \Omega_a \left[|100\rangle(\langle T_1+| \right. \\ &\quad \left. + \langle T_1-|) + |010\rangle(\langle T_2+| + \langle T_2-|) + |001\rangle(\langle T_3+| \right. \\ &\quad \left. + \langle T_3-|) \right] + \text{H.c.} + 2\Omega_b(|D_+\rangle\langle D_+| - |D_-\rangle\langle D_-|) \\ &\quad + \sum_{n=1}^3 \sqrt{2}\Omega_b(|T_{n+}\rangle\langle T_{n+}| - |T_{n-}\rangle\langle T_{n-}|), \end{aligned}$$

where $|D_{\pm}\rangle = (|D_1\rangle \pm |D_2\rangle)/\sqrt{2}$, $|T_{1\pm}\rangle = (|T_1\rangle \pm |1rr\rangle)/\sqrt{2}$, $|T_{2\pm}\rangle = (|T_2\rangle \pm |r1r\rangle)/\sqrt{2}$, and $|T_{3\pm}\rangle = (|T_3\rangle \pm |rr1\rangle)/\sqrt{2}$. According to the above equation, we can find that the effective form of H_{S1}^2 tends to 0 as $\Omega_b \gg \Omega_a$. In other words, the states with three or two atoms at $|0\rangle$ cannot evolve to others by H_{S1}^2 since the corresponding detunings $\pm 2\Omega_b$ or $\pm\sqrt{2}\Omega_b$.

To sum up, the effective Hamiltonian of H_{S1} is $H_{\text{eff1}}^S = H_{S1}^1$, which is the so-called URP in Ref. [52]. Harnessing the similar recipe, we can obtain the effective form of H_{S2} ,

$$H_{\text{eff2}}^S = \Omega_a(|100\rangle\langle r00| + |010\rangle\langle r0r| + |001\rangle\langle r0r|) + \text{H.c.}$$

In light of the switching driving of H_{eff1}^S and H_{eff2}^S , it is obvious that the ground states with one or two atoms at $|0\rangle$ can be pumped into the Rydberg excited states $\{|11r\rangle, |1r1\rangle, |r11\rangle, |r00\rangle, |0r0\rangle, |00r\rangle\}$ that will further decay to the ground states via the spontaneous emission, and only the states $|111\rangle$ and $|000\rangle$ are steady at all times. To intuitively verify the validity of these analyses, we have plotted the dynamical evolution for the populations of $|000\rangle$ and $|111\rangle$ governed by the switching driving of H_{S1} and H_{S2} in Fig. 7. After the alternate operations executed $N = 10$ times, the system beginning with a mixed state is stabilized at the subspace spanned by $\{|000\rangle, |111\rangle\}$ that can be expanded via $\{|\text{GHZ}_+\rangle, |\text{GHZ}_-\rangle\}$. The total population trends towards unit, *i.e.*, $P_{000} + P_{111} = 49.79\% + 49.79\% = 99.58\%$ at $\Omega_b t = 50000$. It faithfully designates the feasibility of the process based on the switching driving of URP.

Besides, the process taking advantage of the Rydberg antiblockade effect makes the state $|\text{GHZ}_+\rangle$ unstable by continuously transferring the state $|+\rangle|+\rangle|+\rangle$ to $|rrr\rangle$. It can be

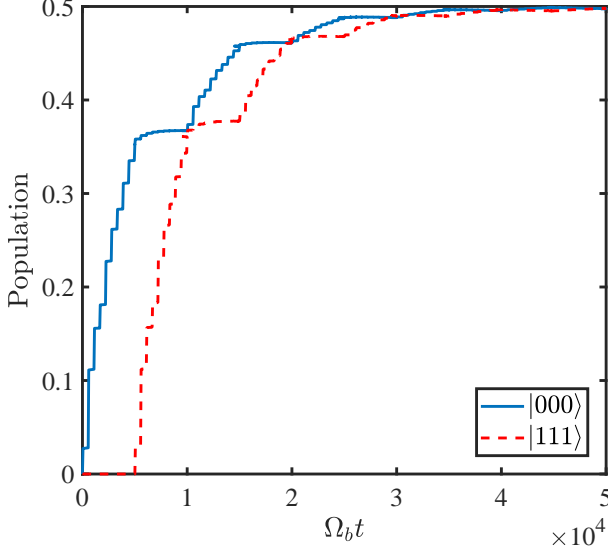


FIG. 7. The dynamical evolution for the populations governed by the switching driving of H_{S_1} and H_{S_2} . The initial state is randomly chosen as a mixed state $\rho_0 = (|100\rangle\langle 100| + |010\rangle\langle 010| + |001\rangle\langle 001| + |011\rangle\langle 011| + |101\rangle\langle 101| + |110\rangle\langle 110|)/6$. The other parameters are $\Omega_a = 0.02\Omega_b$, $\Delta_1 = 300\Omega_b$, $\gamma = 0.01\Omega_b$, and $N = 10$ is the switching number.

indicated by the Hamiltonian H_p . By virtue of the basis $\{|+++ \rangle, |S_1 \rangle, |S_2 \rangle, |rrr \rangle\}$ with $|S_1 \rangle = (|++r \rangle + |r++ \rangle + |r++ \rangle)/\sqrt{3}$ and $|S_2 \rangle = (|+rr \rangle + |r+r \rangle + |rr+ \rangle)/\sqrt{3}$, we can simplify H_p as

$$H_p = \sqrt{6}\Omega_p(|+++ \rangle\langle S_1| + |rrr \rangle\langle S_2|) + 2\sqrt{2}\Omega_p|S_1 \rangle\langle S_2| + \text{H.c.} - \Delta_2|S_1 \rangle\langle S_1| + (U_{pp} - 2\Delta_2)|S_2 \rangle\langle S_2| + (3U_{pp} - 3\Delta_2)|rrr \rangle\langle rrr|. \quad (18)$$

When we suppose $U_{pp} = \Delta_2 \gg \Omega_p$, the Rydberg antiblockade effect is satisfied and the effective form of H_p can be equal to

$$H_{\text{eff}}^p = \frac{12\sqrt{2}\Omega_p^3}{\Delta_2^2}|+++ \rangle\langle rrr| + \text{H.c.}, \quad (19)$$

where we have left out the order of $\mathcal{O}(\Omega_p^2/\Delta_2^2)$ and the Start-shift terms that can be canceled by ancillary levels. Due to the H_{eff}^p , only the state $|+++ \rangle$ can evolve to the state $|rrr \rangle$, which will spontaneously radiate back to the ground states. Then the state $|\text{GHZ}_+\rangle$ is not stable anymore. Meanwhile, combining the Rydberg state decay and the switching driving of H_{S_1} and H_{S_2} , the target state $|\text{GHZ}_-\rangle$ is turned into the unique steady state of the whole system and the second scheme is finished.

B. Numerical results

In Fig. 8, we characterize the fidelity of the target state $|\text{GHZ}_-\rangle$ respectively governed by the full master equation (solid line) and the effective master equation (empty circles)

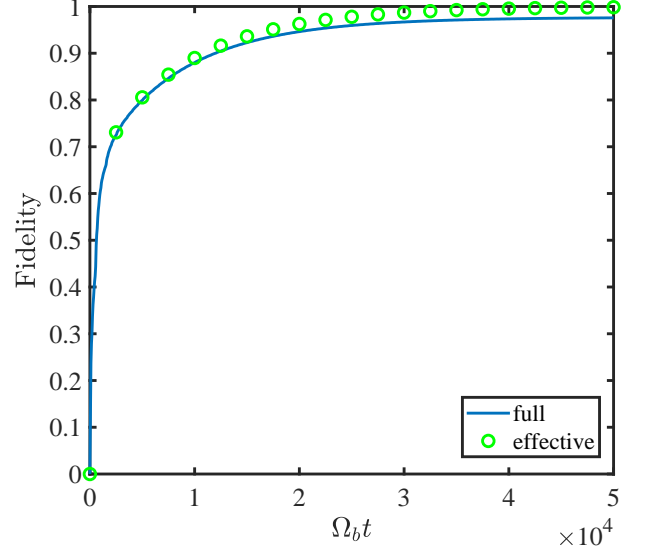


FIG. 8. Fidelity of $|\text{GHZ}_-\rangle$ respectively governed by the full master equation and the effective master equation, where the definition of the fidelity is $F = \text{Tr}[\rho_{\text{GHZ}_-}^{1/2}\rho(t)\rho_{\text{GHZ}_-}^{1/2}]^{1/2}$ and $\rho_{\text{GHZ}_-} = |\text{GHZ}_-\rangle\langle \text{GHZ}_-|$. The initial state is also the mixed state $\rho_0 = (|100\rangle\langle 100| + |010\rangle\langle 010| + |001\rangle\langle 001| + |011\rangle\langle 011| + |101\rangle\langle 101| + |110\rangle\langle 110|)/6$. The other parameters are $\Omega_a = 0.02\Omega_b$, $\Omega_p = \Omega_b$, $\Delta_1 = 300\Omega_b$, $\Delta_2 = 80\Omega_b$, $\gamma = 0.01\Omega_b$, and $N = 64$.

in the interest of exemplifying the correctness for the above derivations, where the effective master equation can be acquired via replacing the $H_{S_{1(2)}} + H_p$ of Eq. (15) (Eq. (16)) with $H_{\text{eff}1(2)}^S + H_{\text{eff}}^p$. The empty circles is in full accord with the curve of the original system, which thoroughly certifies the rationality of the reduced system. Moreover, beginning with a mixed state $\rho_0 = (|100\rangle\langle 100| + |010\rangle\langle 010| + |001\rangle\langle 001| + |011\rangle\langle 011| + |101\rangle\langle 101| + |110\rangle\langle 110|)/6$, the system is successfully stable at the tripartite GHZ state. It means that the present scheme is also independent of the selection of initial state. And evidently different from the previous scheme, the atomic spontaneous emission of the Rydberg states is an important tool. Thus, the fidelity can still arrive at 97.57% with $t = 50000/\Omega_b$ even though the rate of the Rydberg state decay reaches $0.01\Omega_b$.

IV. DISCUSSION AND CONCLUSION

Here, we succinctly explain the generalization of the scheme based on polychromatic driving fields to prepare an arbitrary multipartite GHZ state with odd numbers of atoms. For example, we consider a five-Rydberg-atom system interacts with polychromatic driving fields $\Omega_{1,2,3}$ and a resonant laser Ω_0 . The corresponding atomic energy levels and transitions are the same as those in Fig. 1. But the next-nearest neighbor Rydberg interaction is neglected in the generalized scheme, *i.e.*, the terms of $U_{jk}\sigma_j^{rr}\sigma_k^{rr}$ is replaced with

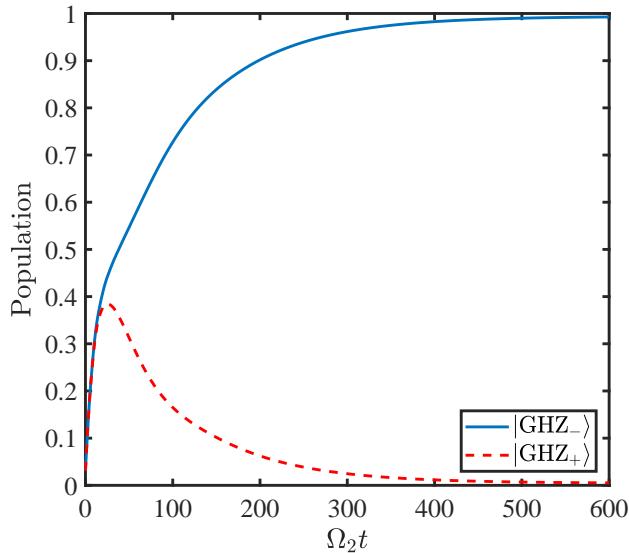


FIG. 9. The dynamical evolution of populations for the five-Rydberg-atom system governed by the effective master equation. The initial state is $\rho_0 = \sum_{l,m,n} P_1^{n_1} P_2^{n_2} P_3^{n_3} P_4^{n_4} P_5^{n_5} / 32$ ($n_{1,2,3,4,5} = 0, 1$). The corresponding parameters are $\Omega_{1,3} = 0.02\Omega_2$ and $\Gamma_{\text{eff}} = 0.4\Omega_2$.

$U_{j,j+1}\sigma_j^{rr}\sigma_{j+1}^{rr}$. In the same conditions, $U_{j,j+1} = U = \Delta_2 = (\Delta_3 + \Delta_1)/2 \gg \Omega_{0,1,2,3}$ and $\Gamma \gg \Omega_0$, a Hamiltonian similar to the H_r of Eq. (2) and the engineered spontaneous emissions $L_{\text{eff}}^j = \sqrt{\Gamma_{\text{eff}}} P_{j-1}^0 \sigma_j^{gr} P_{j+1}^0$ can be derived. To guarantee the target state $|GHZ_-\rangle = (|0\rangle^{\otimes 5} - |r\rangle^{\otimes 5})/\sqrt{2}$ is the unique steady state of the system, it is the heart to set $\Delta_1 = (1 + \sqrt{5})\Omega_2$ which is equal to one of the eigenvalues with respect to the resonant terms of H_r of the five-Rydberg-atom system. Then we can obtain an effective Hamiltonian analogous to the Eq. (13) in the regime of large detuning $\Omega_2 \gg \Omega_{1,3}$.

In Fig. 9, we plot the dynamical evolution of populations for the five-Rydberg-atom system governed by the effective master equation. The feasibility of the generalized scheme is fully attested through the populations of $|GHZ_-\rangle$ (solid line) and $|GHZ_+\rangle$ (dashed line) respectively arriving at 99.27% and 0.53% with $\Omega_2 t = 600$. Besides, the generalized scheme needn't the certain transport time or the tailored initial state, either.

Finally, we investigate the experimental feasibility. To date, it is an available experimental technology to arrange a group of Rydberg atoms into various geometries [67–70]. Furthermore, Gaëtan *et al.* [71] demonstrated the Rydberg interaction can be kept up to $U = 2\pi \times 50$ MHz between two Rydberg atoms individually trapped in optical tweezers at a distance of 4 μm . And in view of this proposal, Müller *et al.* [72] utilized two Rydberg atoms in spatially separated dipole

traps at a distance of 0.3 μm to obtain a Rydberg interaction $U = 2\pi \times 118$ GHz and implement a controlled- Z gate. Therefore, we consider the distance of the Rydberg atoms in our scheme can be varied in [0.3, 4] μm to select appropriate strengths for the interactions. In addition, the experimental realization for the couplings between the ground states and the Rydberg states actually needs a two-step transition [14, 71], where the ground state and the Rydberg state will directly couple to an intermediate state dispersively. In the regime of large detuning, one can obtain the equivalent direct transition from the ground state to the Rydberg state by adiabatically eliminating the intermediate state. Accordingly, the equivalent Rabi frequency corresponding to the Ω_α ($\alpha = 1, 2, 3, a, b, p$) in our scheme can be continuously tuned by the programmable Rabi frequencies and detunings of the two-step transition. Referring to the Ref. [73–75], the decay rate of the temporary state and Rydberg states can be regarded as $\Gamma = 2\pi \times 5.75$ MHz (or $2\pi \times 6.1$ MHz) and $\gamma = 2\pi \times 0.03$ MHz. In accordance with these analyses, the relationships between the relevant parameters of Fig. 2 and Fig. 8 are still practicable while $(\Omega_2, \Gamma) = 2\pi \times (1, 5.75)$ MHz and $(\Omega_b, \gamma) = 2\pi \times (3, 0.03)$ MHz. These reflect the experimental feasibility of the above two schemes.

To conclude, we have elaborately designed two dissipative schemes to prepare the tripartite GHZ state in a neutral atom system. In the first scheme, the GHZ states with odd numbers of atoms are successfully generated in a very short time by the organic combination between the Rydberg antiblockade effect resulting from the polychromatic driving fields and the engineered spontaneous emission induced by a temporary level. However, the first scheme is sensitive to the spontaneous emission of the Rydberg states. Therefore, in the second scheme, benefitting from the cooperation between the switching driving of unconventional Rydberg pumping caused by dichromatic driving fields and the Rydberg antiblockade effect, the spontaneous emission of the Rydberg states is characterized as a significant resource to realize the generation of the tripartite GHZ state. And the fidelity of the target state can be around 98% via the state-of-the-art technology. Furthermore, because the target state is the unique steady-state solution for the whole system, the two scenarios both possess the special superiorities of dissipative entangled-state preparations, *i.e.*, they never require to precisely control the transport time or exactly tailor the initial state. We believe our schemes supply a viable prospect with regard to preparations of multipartite GHZ states.

ACKNOWLEDGMENTS

This work is supported by National Natural Science Foundation of China (NSFC) under Grants No. 11774047.

[1] M. Saffman, T. G. Walker, and K. Mølmer, “Quantum information with rydberg atoms,” *Rev. Mod. Phys.* **82**, 2313 (2010).

[2] Y. O. Dudin and A. Kuzmich, “Strongly interacting rydberg excitations of a cold atomic gas,” *Science* **336**, 887 (2012).

- [3] J. Lampen, H. Nguyen, L. Li, P. R. Berman, and A. Kuzmich, “Long-lived coherence between ground and rydberg levels in a magic-wavelength lattice,” *Phys. Rev. A* **98**, 033411 (2018).
- [4] H. Weimer, M. Muller, I. Lesanovsky, P. Zoller, and H. P. Buchler, “A rydberg quantum simulator,” *Nat. Phys.* **6**, 382–388 (2010).
- [5] C. J. Turner, A. A. Michailidis, D. A. Abanin, M. Serbyn, and Z. Papić, “Weak ergodicity breaking from quantum many-body scars,” *Nat. Phys.* **14**, 745 (2018).
- [6] A. Pífeiro Orioli, A. Signoles, H. Wildhagen, G. Günter, J. Berges, S. Whitlock, and M. Weidemüller, “Relaxation of an isolated dipolar-interacting rydberg quantum spin system,” *Phys. Rev. Lett.* **120**, 063601 (2018).
- [7] Vittorio Giovannetti, Seth Lloyd, and Lorenzo Maccone, “Advances in quantum metrology,” *Nat. Photonics* **5**, 222 (2011).
- [8] Adrien Facon, Eva-Katharina Dietsche, Dorian Grosso, Serge Haroche, Jean-Michel Raimond, Michel Brune, and Sébastien Gleyzes, “A sensitive electrometer based on a rydberg atom in a schrödinger-cat state,” *Nature* **535**, 262 (2016).
- [9] C. L. Degen, F. Reinhard, and P. Cappellaro, “Quantum sensing,” *Rev. Mod. Phys.* **89**, 035002 (2017).
- [10] A. Arias, G. Lochead, T. M. Wintermantel, S. Helmrich, and S. Whitlock, “Realization of a rydberg-dressed ramsay interferometer and electrometer,” *Phys. Rev. Lett.* **122**, 053601 (2019).
- [11] D. Jaksch, J. I. Cirac, P. Zoller, S. L. Rolston, R. Côté, and M. D. Lukin, “Fast quantum gates for neutral atoms,” *Phys. Rev. Lett.* **85**, 2208–2211 (2000).
- [12] E. Urban, T. A. Johnson, T. Henage, L. Isenhower, D. D. Yavuz, T. G. Walker, and M. Saffman, “Observation of rydberg blockade between two atoms,” *Nat. Phys.* **5**, 110 (2009).
- [13] M. Saffman and K. Mølmer, “Efficient multiparticle entanglement via asymmetric rydberg blockade,” *Phys. Rev. Lett.* **102**, 240502 (2009).
- [14] T. Wilk, A. Gaëtan, C. Evellin, J. Wolters, Y. Miroshnychenko, P. Grangier, and A. Browaeys, “Entanglement of two individual neutral atoms using rydberg blockade,” *Phys. Rev. Lett.* **104**, 010502 (2010).
- [15] D. D. Bhaktavatsala Rao and K. Mølmer, “Dark entangled steady states of interacting rydberg atoms,” *Phys. Rev. Lett.* **111**, 033606 (2013).
- [16] I. I. Beterov, G. N. Hamzina, E. A. Yakshina, D. B. Tretyakov, V. M. Entin, and I. I. Ryabtsev, “Adiabatic passage of radio-frequency-assisted förster resonances in rydberg atoms for two-qubit gates and the generation of bell states,” *Phys. Rev. A* **97**, 032701 (2018).
- [17] A.-X. Chen, “Implementation of deutsch-jozsa algorithm and determination of value of function via rydberg blockade,” *Opt. Express* **19**, 2037 (2011).
- [18] Y. Han, B. He, K. Heshami, C.-Z. Li, and C. Simon, “Quantum repeaters based on rydberg-blockade-coupled atomic ensembles,” *Phys. Rev. A* **81**, 052311 (2010).
- [19] C. Ates, T. Pohl, T. Pattard, and J. M. Rost, “Antiblockade in rydberg excitation of an ultracold lattice gas,” *Phys. Rev. Lett.* **98**, 023002 (2007).
- [20] T. Amthor, C. Giese, C. S. Hofmann, and M. Weidemüller, “Evidence of antiblockade in an ultracold rydberg gas,” *Phys. Rev. Lett.* **104**, 013001 (2010).
- [21] S. L. Su, H. Z. Shen, Erjun Liang, and Shou Zhang, “One-step construction of the multiple-qubit rydberg controlled-phase gate,” *Phys. Rev. A* **98**, 032306 (2018).
- [22] S.-L. Su, Fu-Qiang Guo, L. Tian, X.-Y. Zhu, L.-L. Yan, E.-J. Liang, and M. Feng, “Nondestructive rydberg parity meter and its applications,” *Phys. Rev. A* **101**, 012347 (2020).
- [23] A. W. Carr and M. Saffman, “Preparation of entangled and antiferromagnetic states by dissipative rydberg pumping,” *Phys. Rev. Lett.* **111**, 033607 (2013).
- [24] S.-L. Su, Y. Tian, H. Z. Shen, H. Zang, E. Liang, and S. Zhang, “Applications of the modified rydberg antiblockade regime with simultaneous driving,” *Phys. Rev. A* **96**, 042335 (2017).
- [25] J. Song, C. Li, Z.-J. Zhang, Y.-Y. Jiang, and Y. Xia, “Implementing stabilizer codes in noisy environments,” *Phys. Rev. A* **96**, 032336 (2017).
- [26] D.-X. Li, X.-Q. Shao, J.-H. Wu, and X. X. Yi, “Dissipation-induced w state in a rydberg-atom-cavity system,” *Opt. Lett.* **43**, 1639 (2018).
- [27] D. X. Li and X. Q. Shao, “Directional quantum state transfer in a dissipative rydberg-atom-cavity system,” *Phys. Rev. A* **99**, 032348 (2019).
- [28] Ryszard Horodecki, Paweł Horodecki, Michał Horodecki, and Karol Horodecki, “Quantum entanglement,” *Rev. Mod. Phys.* **81**, 865 (2009).
- [29] Robert Raussendorf and Hans J. Briegel, “A one-way quantum computer,” *Phys. Rev. Lett.* **86**, 5188 (2001).
- [30] Masahito Hayashi and Tomoyuki Morimae, “Verifiable measurement-only blind quantum computing with stabilizer testing,” *Phys. Rev. Lett.* **115**, 220502 (2015).
- [31] Mariami Gachechiladze, Otfried Gühne, and Akimasa Miyake, “Changing the circuit-depth complexity of measurement-based quantum computation with hypergraph states,” *Phys. Rev. A* **99**, 052304 (2019).
- [32] D. Gottesman, “Stabilizer codes and quantum error correction,” *ArXiv e-prints* 970502 (1997).
- [33] D. Schlingemann and R. F. Werner, “Quantum error-correcting codes associated with graphs,” *Phys. Rev. A* **65**, 012308 (2001).
- [34] Mark Hillery, Vladimír Bužek, and André Berthiaume, “Quantum secret sharing,” *Phys. Rev. A* **59**, 1829 (1999).
- [35] W. McCutcheon, A. Pappa, B. A. Bell, A. McMillan, A. Chailoux, T. Lawson, M. Mafu, D. Markham, E. Diamanti, I. Kerenidis, J. G. Rarity, and M. S. Tame, “Experimental verification of multipartite entanglement in quantum networks,” *Nat. Commun.* **7**, 13251 (2016).
- [36] Ahmed Farouk, J. Batle, M. Elhoseny, Mosayeb Naseri, Muzaffar Lone, Alex Fedorov, Majid Alkhambashi, Syed Hassan Ahmed, and M. Abdel-Aty, “Robust general n user authentication scheme in a centralized quantum communication network via generalized ghz states,” *Front. Phys.* **13**, 130306 (2018).
- [37] F. Verstraete, V. Murg, and J.I. Cirac, “Matrix product states, projected entangled pair states, and variational renormalization group methods for quantum spin systems,” *Adv. Phys.* **57**, 143 (2008).
- [38] Román Orús, “A practical introduction to tensor networks: Matrix product states and projected entangled pair states,” *Ann. Phys.* **349**, 117 (2014).
- [39] Jian-Wei Pan, Zeng-Bing Chen, Chao-Yang Lu, Harald Weinfurter, Anton Zeilinger, and Marek Żukowski, “Multiphoton entanglement and interferometry,” *Rev. Mod. Phys.* **84**, 777 (2012).
- [40] D. M. Greenberger, M.A. Horne, and A. Zeilinger, “Bell’s theorem, quantum theory, and conceptions of the universe,” (Kluwer Academic, Dordrecht, 1989) pp. 69–72.
- [41] Tetsufumi Tanamoto, Yu-xi Liu, Shinobu Fujita, Xuedong Hu, and Franco Nori, “Producing cluster states in charge qubits and flux qubits,” *Phys. Rev. Lett.* **97**, 230501 (2006).
- [42] Ying Li, Peter C. Humphreys, Gabriel J. Mendoza, and Simon C. Benjamin, “Resource costs for fault-tolerant linear optical quantum computing,” *Phys. Rev. X* **5**, 041007 (2015).

- [43] Vittorio Giovannetti, Seth Lloyd, and Lorenzo Maccone, “Quantum-enhanced measurements: Beating the standard quantum limit,” *Science* **306**, 1330 (2004).
- [44] W. Dür, M. Skotiniotis, F. Fröwis, and B. Kraus, “Improved quantum metrology using quantum error correction,” *Phys. Rev. Lett.* **112**, 080801 (2014).
- [45] Luca Pezzè, Augusto Smerzi, Markus K. Oberthaler, Roman Schmied, and Philipp Treutlein, “Quantum metrology with nonclassical states of atomic ensembles,” *Rev. Mod. Phys.* **90**, 035005 (2018).
- [46] J. J. Bollinger, Wayne M. Itano, D. J. Wineland, and D. J. Heinzen, “Optimal frequency measurements with maximally correlated states,” *Phys. Rev. A* **54**, R4649 (1996).
- [47] S. F. Huelga, C. Macchiavello, T. Pellizzari, A. K. Ekert, M. B. Plenio, and J. I. Cirac, “Improvement of frequency standards with quantum entanglement,” *Phys. Rev. Lett.* **79**, 3865 (1997).
- [48] F. Reiter, D. Reeb, and A. S. Sørensen, “Scalable dissipative preparation of many-body entanglement,” *Phys. Rev. Lett.* **117**, 040501 (2016).
- [49] X. Q. Shao, J. H. Wu, X. X. Yi, and Gui-Lu Long, “Dissipative preparation of steady greenberger-horne-zeilinger states for rydberg atoms with quantum zeno dynamics,” *Phys. Rev. A* **96**, 062315 (2017).
- [50] A. Omran, H. Levine, A. Keesling, G. Semeghini, T. T. Wang, S. Ebadi, H. Bernien, A. S. Zibrov, H. Pichler, S. Choi, J. Cui, M. Rossignolo, P. Rembold, S. Montangero, T. Calarco, M. Endres, M. Greiner, V. Vuletić, and M. D. Lukin, “Generation and manipulation of schrödinger cat states in rydberg atom arrays,” *Science* **365**, 570 (2019).
- [51] Dong-Xiao Li, Tai-Yu Zheng, and Xiao-Qiang Shao, “Adiabatic preparation of multipartite ghz states via rydberg ground-state blockade,” *Opt. Express* **27**, 20874 (2019).
- [52] D. X. Li and X. Q. Shao, “Unconventional rydberg pumping and applications in quantum information processing,” *Phys. Rev. A* **98**, 062338 (2018).
- [53] T. M. Wintermantel, Y. Wang, G. Lochead, S. Shevate, G. K. Brennen, and S. Whitlock, “Unitary and nonunitary quantum cellular automata with rydberg arrays,” *Phys. Rev. Lett.* **124**, 070503 (2020).
- [54] T. G. Walker and M. Saffman, “Consequences of zeeman degeneracy for the van der waals blockade between rydberg atoms,” *Phys. Rev. A* **77**, 032723 (2008).
- [55] Y.-M. Liu, X.-D. Tian, D. Yan, Y. Zhang, C.-L. Cui, and J.-H. Wu, “Nonlinear modifications of photon correlations via controlled single and double rydberg blockade,” *Phys. Rev. A* **91**, 043802 (2015).
- [56] Anders Sørensen and Klaus Mølmer, “Quantum computation with ions in thermal motion,” *Phys. Rev. Lett.* **82**, 1971 (1999).
- [57] Daniel Jonathan and Martin B. Plenio, “Light-shift-induced quantum gates for ions in thermal motion,” *Phys. Rev. Lett.* **87**, 127901 (2001).
- [58] Shi-Biao Zheng, “Quantum logic gates for hot ions without a speed limitation,” *Phys. Rev. Lett.* **90**, 217901 (2003).
- [59] K. J. Engel and R. Nagel, *One-Parameter Semigroups for Linear Evolution Equations* (Springer, New York, 2000).
- [60] József Zsolt Bernád and Juan Mauricio Torres, “Partly invariant steady state of two interacting open quantum systems,” *Phys. Rev. A* **92**, 062114 (2015).
- [61] X. X. Li, H. D. Yin, D. X. Li, and X. Q. Shao, “Deterministic generation of maximally discordant mixed states by dissipation,” *Phys. Rev. A* **101**, 012329 (2020).
- [62] Klaus Mølmer and Anders Sørensen, “Multiparticle entanglement of hot trapped ions,” *Phys. Rev. Lett.* **82**, 1835 (1999).
- [63] Xiao-Qiang Shao, “Engineering steady entanglement for trapped ions at finite temperature by dissipation,” *Phys. Rev. A* **98**, 042310 (2018).
- [64] L. Allan and J. M. Eberly, *Optical Resonance and TwoLevel Atoms* (Dover, New York, 1987).
- [65] Fazal Badshah, Muhammad Irfan, Sajid Qamar, and Shahid Qamar, “Coherent control of tunneling and traversal of ultracold atoms through vacuum-induced potentials,” *Phys. Rev. A* **88**, 044101 (2013).
- [66] Ran Cheng, Matthew W. Daniels, Jian-Gang Zhu, and Di Xiao, “Ultrafast switching of antiferromagnets via spin-transfer torque,” *Phys. Rev. B* **91**, 064423 (2015).
- [67] D. W. Schönleber, A. Eisfeld, M. Genkin, S. Whitlock, and S. Wüster, “Quantum simulation of energy transport with embedded rydberg aggregates,” *Phys. Rev. Lett.* **114**, 123005 (2015).
- [68] Daniel Barredo, Sylvain de Léséleuc, Vincent Lienhard, Thierry Lahaye, and Antoine Browaeys, “An atom-by-atom assembler of defect-free arbitrary two-dimensional atomic arrays,” *Science* **354**, 1021 (2016).
- [69] Manuel Endres, Hannes Bernien, Alexander Keesling, Harry Levine, Eric R. Anschuetz, Alexandre Krajenbrink, Crystal Senko, Vladan Vuletic, Markus Greiner, and Mikhail D. Lukin, “Atom-by-atom assembly of defect-free one-dimensional cold atom arrays,” *Science* **354**, 1024 (2016).
- [70] D. W. Schönleber, C. D. B. Bentley, and A. Eisfeld, “Engineering thermal reservoirs for ultracold dipole-dipole-interacting rydberg atoms,” *New J. Phys.* **20**, 013011 (2018).
- [71] Alpha Gaëtan, Yevhen Miroshnychenko, Tatjana Wilk, Amodsen Chotia, Matthieu Viteau, Daniel Comparat, Pierre Pillet, Antoine Browaeys, and Philippe Grangier, “Observation of collective excitation of two individual atoms in the rydberg blockade regime,” *Nat. Phys.* **5**, 115 (2009).
- [72] Matthias M. Müller, Michael Murphy, Simone Montangero, Tommaso Calarco, Philippe Grangier, and Antoine Browaeys, “Implementation of an experimentally feasible controlled-phase gate on two blockaded rydberg atoms,” *Phys. Rev. A* **89**, 032334 (2014).
- [73] Y. Miroshnychenko, A. Gaëtan, C. Evellin, P. Grangier, D. Comparat, P. Pillet, T. Wilk, and A. Browaeys, “Coherent excitation of a single atom to a rydberg state,” *Phys. Rev. A* **82**, 013405 (2010).
- [74] A Grankin, E Brion, E Bimbard, R Boddeda, I Usmani, A Ourjoumtsev, and P Grangier, “Quantum statistics of light transmitted through an intracavity rydberg medium,” *New J. Phys.* **16**, 043020 (2014).
- [75] S. Whitlock, H. Wildhagen, H. Weimer, and M. Weidemüller, “Diffusive to nonergodic dipolar transport in a dissipative atomic medium,” *Phys. Rev. Lett.* **123**, 213606 (2019).